Nb_9PdAs_7: A Unique Arrangement in the $M_{n^2+3n+2}X_{n^2+n}Y$ Family of Hexagonal Structures

Meitian Wang and Arthur Mar*

Department of Chemistry, University of Alberta, Edmonton, Alberta, Canada T6G 2G2

Received May 23, 2001

The ternary transition-metal arsenide Nb_9PdAs_7 has been prepared through reaction of the elements, and its structure has been determined by single-crystal X-ray diffraction methods. It adopts a new structure type (Pearson symbol *hP*51, hexagonal, space group $P\bar{6}$, $Z = 3$), with unit cell parameters $a = 16.6955(6)$ and $c = 3.5582(1)$ Å. The structure contains assemblies of As-centered trigonal prisms that extend as triangular columns through sharing of the triangular faces. Not only does Nb_9PdAs_7 extend a family of hexagonal structures with general formula $M_{n^2+3n+2}X_{n^2+n}Y$ to $n = 4$, the highest member known thus far, but it also displays the unique feature in which there are two distinct types of triangular columns, one having corner atoms (Pd) different from the other atoms (Nb). Structural relationships between members of the $M_{n^2+3n+2}X_{n^2+n}Y$ family are presented. The chemical bonding in Nb_9PdAs_7 was analyzed through an extended Hückel band structure calculation.

Introduction

Binary transition metal−pnicogen (M−Pn) compounds have been studied extensively and can be classified into pnicogen-rich or metal-rich phases.[1,2] The structures of most pnicogen-rich phases, which may involve substantial nonmetal−nonmetal bonding in nonclassical patterns, can be interpreted surprisingly well by the simple Zintl concept.[3] Our understanding of metal-rich phases remains poor, although it is apparent that homoatomic metal−metal bonding, in addition to the strong metal−pnicogen bonding component, plays an important role in stabilizing these compounds.

There is now a growing body of examples of ternary pnictides containing two transition metals. For combinations of early (EM) and late transition metals (LM), the vast majority of these contain Ni.[4] In pnicogen-rich ternary compounds such as $MNiPn_2$ (M = Zr, Hf; Pn = P, As),[4a,d] ordered structures are observed because EM and LM prefer different coordination environments; the same principle is operative in the structures of many ternary chalcogenides[5] or halides.[6] In metal-rich ternary compounds, such as $M_3Pd_4P_3$ or $M_5Pd_9P_7$ (M = Zr, Hf),[4a,b] metal−metal interactions become increasingly important so that ordered structures are equally found, not only because of the different coordination preferences, but also because of the drive to maximize the Lewis acid−base stabilization derived from strong heteroatomic EM−LM interactions (involving donation of electron density to EM from LM),[7] which can be supplemented by homoatomic EM−EM and LM−LM interactions as well. For combinations of two EM, it might not be thought that new structure types or ordered structures would result from metals with similar coordination preferences. Nevertheless, such compounds as $Zr_{6.45}Nb_{4.55}P_4$[8] adopt structures not found in the corresponding binary phases and display differential fractional site occupancy (DFSO).[9]

Our primary interest is in the metal-rich regions of the ternary systems (Zr, Hf, Nb, Ta)−(Ni, Pd, Pt)−(P, As, Sb).[4] The systems containing a group 4 metal have been studied fairly comprehensively, although compounds with new structure types such as $Zr_9Ni_2P_4$,[10] Hf_5NiP_3,[11] $M_3Pd_4P_3$ (M = Zr, Hf),[4a] and $M_5Pd_9P_7$ (M = Zr, Hf)[4b] are still being found. The systems containing a group 5 metal have been most well studied in conjunction with Ni. There are thirteen compounds found in the (Nb, Ta)−Ni−P system and three compounds in the (Nb, Ta)−Ni−As system.[4] All of them are metal-rich, containing substantial metal−metal bonding in their structures but no Pn−

* To whom correspondence should be addressed. Telephone: (780) 492-5592. Fax: (780) 492-8231. E-mail: arthur.mar@ualberta.ca.

(1) Hulliger, F. In *Structure and Bonding*; Jørgensen, C. K., Neilands, J. B., Nyholm, R. S., Reinen, D., Williams, R. J. P., Eds.; Springer-Verlag: New York, 1968; Vol. 4, p 83.
(2) Villars, P. *Pearson's Handbook, Desk Edition*; ASM International: Materials Park, OH, 1997.
(3) Papoian, G. A.; Hoffmann, R. *Angew. Chem., Int. Ed.* **2000**, *39*, 2408.
(4) (a) $M_3Pd_4P_3$ (M = Zr, Hf), HfPdSb, $Nb_5Pd_4P_4$: Wang, M.; McDonald, R.; Mar, A. *Inorg. Chem.* **2000**, *39*, 4936. $M_xNi_yP_z$ (M = Zr, Hf, Nb, Ta): see references therein. (b) $M_5Pd_9P_7$ (M = Zr, Hf), ZrPdAs, ZrPdSb: Heerdmann, A.; Johrendt, D.; Mewis, A. *Z. Anorg. Allg. Chem.* **2000**, *626*, 1393. (c) ZrNiAs, HfNiAs: Kleinke, H.; Franzen, H. F. *Z. Anorg. Allg. Chem.* **1998**, *624*, 51. (d) $ZrNi_{0.75}As_2$, $HfNi_{0.75}As_2$: El Ghadraoui, E. H.; Pivan, J. Y.; Guérin, R. *J. Less-Common Met.* **1988**, *136*, 303. (e) Zr_2NiAs_2: El Ghadraoui, E. H.; Pivan, J. Y.; Guérin, R.; Sergent, M. *Mater. Res. Bull.* **1988**, *23*, 891. (f) $ZrNi_4As_2$, $HfNi_4As_2$: Pivan, J. Y.; Guérin, R.; El Ghadraoui, E. H.; Rafiq, M. *J. Less-Common Met.* **1989**, *153*, 285. (g) $Zr_2Ni_3As_3$, $Hf_2Ni_3As_3$: El Ghadraoui, E. H.; Pivan, J. Y.; Guérin, R.; Padiou, J.; Sergent, M. *J. Less-Common Met.* **1985**, *105*, 187. (h) NbNiAs, TaNiAs: Rundqvist, S.; Tansuriwongs, P. *Acta Chem. Scand.* **1967**, *21*, 813. (i) $NbNiAs_2$: El Ghadraoui, E. H.; Guérin, R.; Padiou, J.; Sergent, M. *C. R. Seances Acad. Sci., Ser. 2* **1983**, *296*, 617. (j) ZrNiSb, HfNiSb: Kleinke, H. *Z. Anorg. Allg. Chem.* **1998**, *624*, 1272. (k) $ZrNi_2Sb$, $HfNi_2Sb$: Dwight, A. E. *Mater. Res. Bull.* **1987**, *22*, 201. (l) Zr_5NiSb_3: Garcia, E.; Corbett, J. D. *Inorg. Chem.* **1990**, *29*, 3274. (m) $Zr_5Ni_{0.5}Sb_{2.5}$: Kwon, Y.-U.; Sevov, S. C.; Corbett, J. D. *Chem. Mater.* **1990**, *2*, 550. (n) $Zr_3Ni_3Sb_4$, $Hf_3Ni_3Sb_4$, $Zr_3Pt_3Sb_4$: Wang, M.; McDonald, R.; Mar, A. *Inorg. Chem.* **1999**, *38*, 3435. (o) Zr_6NiSb_2, Hf_6NiSb_2: Melnyk, G.; Bauer, E.; Rogl, P.; Skolozdra, R.; Seidl, E. *J. Alloys Compd.* **2000**, *296*, 235. (p) Hf_5NiSb_3: Rieger, W.; Parthé, E. *Acta Crystallogr., Sect. B: Struct. Crystallogr. Cryst. Chem.* **1968**, *24*, 456. (q) $Hf_6Ni_{1-x}Sb_{2+x}$: Kleinke, H. *J. Alloys Compd.* **1998**, *270*, 136. (r) $Hf_{10}Ni_xSb_{6-x}$: Kleinke, H.; Ruckert, C.; Felser, C. *Eur. J. Inorg. Chem.* **2000**, 315. (s) $Nb_{28}Ni_{33.5}Sb_{12.5}$: Wang, M.; Mar, A. *J. Solid State Chem.*, in press.
(5) Hughbanks, T. *J. Alloys Compd.* **1995**, *229*, 40.
(6) Corbett, J. D. *J. Alloys Compd.* **1995**, *229*, 10.
(7) Brewer, L.; Wengert, P. R. *Metall. Trans.* **1973**, *4*, 83.
(8) Marking, G. A.; Franzen, H. F. *Chem. Mater.* **1993**, *5*, 678.
(9) Franzen, H. F.; Köckerling, M. *Prog. Solid State Chem.* **1995**, *23*, 265.
(10) Kleinke, H.; Franzen, H. F. *Inorg. Chem.* **1996**, *35*, 5272.
(11) Kleinke, H.; Franzen, H. F. *Chem. Mater.* **1997**, *9*, 1030.

10.1021/ic010544h CCC: $20.00
Published on Web 09/05/2001

Pn bonding (except in $NbNiP_2$, $TaNiP_2$, and $NbNiAs_2$,[4i] possessing the $UMoC_2$-type structure, which have weak ~2.79 Å P−P or ~2.95 Å As−As bonds). Recently discovered $Nb_{28}Ni_{33.5}Sb_{12.5}$ is the first compound found in the (Nb, Ta)−Ni−Sb system.[4s] To our knowledge, so far $Nb_5Pd_4P_4$[4a] has been the only compound found in the (Nb, Ta)−Pd−(P, As, Sb) systems, and none has been found in the (Nb, Ta)−Pt−(P, As, Sb) systems.

Reported here are the preparation, structure, bonding, and resistivity of Nb_9PdAs_7, the first compound found in the (Nb, Ta)−Pd−As systems. Like many other ternary pnictides, pnicogen-centered trigonal prisms serve as the building blocks, but the arrangement is quite unusual in Nb_9PdAs_7, and its structure type, which is new, belongs to a missing member of a family of hexagonal structures with the general formula $M_{n^2+3n+2}X_{n^2+n}Y$.[12]

Experimental Section

Synthesis. Binary NbAs was first prepared by the direct reaction of stoichiometric amounts of the elemental powders (Nb, 99.8%, Cerac; As, 99.99%, Alfa-Aesar) in an evacuated fused-silica tube heated at 500 °C for 2 days and 1000 °C for 3 days. A 0.25 g mixture of Pd (99.95%, Alfa-Aesar) and NbAs in a 1:1 molar ratio was pressed into a pellet and arc-melted in a Centorr 5TA tri-arc furnace under argon (gettered by melting a titanium pellet). Some needle-shaped crystals were found which contained all three elements on the basis of EDX (energy-dispersive X-ray) analysis on a Hitachi S-2700 scanning electron microscope. Because these crystals were rather small, insufficient X-ray diffraction intensity prevented satisfactory completion of a structure refinement. Nevertheless, a preliminary structure determination suggested two reasonable possibilities for the composition, "$Nb_{27}Pd_3As_{21}$ (Nb_9PdAs_7)" or "$Nb_{24}Pd_6As_{21}$ ($Nb_8Pd_2As_7$)".

To promote better crystal growth, a few grains of iodine were added in two reactions of Nb, Pd, and As in 27:3:21 and 24:6:24 molar ratios carried out in fused-silica tubes in a two-zone furnace heated in a temperature gradient of 1000/1050 °C (charge in cool zone) for 3 days. Both reactions now gave larger crystals which contained 56% Nb, 4% Pd, and 40% As (average of 11 crystals), as determined from EDX analysis. One of these crystals was chosen for the ultimate structure determination.

Finally, the three reactions (i) 27 Nb + 3 Pd + 21 As, (ii) 24 Nb + 6 Pd + 21 As, and (iii) 30 Nb + 21 As were carried out in alumina tubes jacketed by fused-silica tubes heated at 1000 °C for 3 days. On the basis of X-ray powder diffraction patterns obtained on an Enraf-Nonius FR552 Guinier camera (Cu $K\alpha_1$ radiation), reaction i produced the desired hexagonal phase essentially quantitatively, reaction ii produced the desired hexagonal phase and other binary phases, and reaction iii produced only binary NbAs and Nb_5As_3. The EDX analysis, the results of these reactions, and the single-crystal structure determination strongly support the conclusion that the correct composition of the hexagonal phase is $Nb_{27}Pd_3As_{21}$ (or Nb_9PdAs_7) and that it is not another new binary Nb−As phase.

Structure Determination. Weissenberg photography confirmed the singularity of the selected needle-shaped crystal and gave preliminary cell parameters. X-ray diffraction data were collected on a Bruker Platform/SMART 1000 CCD diffractometer at room temperature (22 °C) using ω scans (0.2°) in the range $2.82° \le 2\theta$ (Mo $K\alpha$) $\le 65.14°$. Final cell parameters were refined from least-squares analysis of 3161 reflections. Crystal data and further details of the data collection are given in Table 1. All calculations were carried out with use of the SHELXTL (version 5.1) package.[13] Conventional atomic scattering factors and anomalous dispersion corrections were used.[14] Intensity data were processed, and face-indexed numerical absorption corrections were applied in XPREP.

Table 1. Crystallographic Data for Nb_9PdAs_7

fw 1467.03	$T = 22$ °C
space group $C_{3h}^1 - P\bar{6}$ (No. 174)	$\lambda = 0.710\ 73$ Å
$a = 16.6955(6)$ Å[a]	$\rho_{calcd} = 8.508$ g cm^{-3}
$c = 3.5582(1)$ Å[a]	μ (Mo Kα)= 302.01 cm^{-1}
$V = 858.93(5)$ Å^3 [a]	$R(F)$ for $F_o^2 > 2\sigma(F_o^2) = 0.033$[b]
$Z = 3$	$R_w(F_o^2) = 0.073$[c]

[a] Obtained from a refinement constrained so that $a = b$, $\alpha = \beta = 90°$, and $\gamma = 120°$. [b] $R(F) = \sum||F_o| - |F_c||/\sum|F_o|$. [c] $R_w(F_o^2) = [\sum[w(F_o^2 - F_c^2)^2]/\sum wF_o^4]^{1/2}$; $w^{-1} = [\sigma^2(F_o^2) + (0.0208\ p)^2 + 0.3365\ p]$, where $p = [\max(F_o^2, 0) + 2F_c^2]/3$.

Table 2. Positional and Equivalent Isotropic Displacement Parameters for Nb_9PdAs_7

atom	Wyckoff position	x	y	z	U_{eq} (Å^2)[a]
Nb(1)	3*k*	0.31536(10)	0.20192(9)	1/2	0.0030(3)
Nb(2)	3*k*	0.35787(9)	0.02973(9)	1/2	0.0037(3)
Nb(3)	3*k*	0.53364(9)	0.24556(9)	1/2	0.0033(3)
Nb(4)	3*k*	0.57828(10)	0.07225(10)	1/2	0.0032(3)
Nb(5)	3*j*	0.07269(10)	0.49636(10)	0	0.0029(3)
Nb(6)	3*j*	0.11658(9)	0.31844(9)	0	0.0036(3)
Nb(7)	3*j*	0.13091(9)	0.12059(9)	0	0.0065(3)
Nb(8)	3*j*	0.28785(9)	0.53367(9)	0	0.0025(3)
Nb(9)	3*j*	0.32442(9)	0.35451(9)	0	0.0028(3)
Pd	3*k*	0.01025(8)	0.15826(8)	1/2	0.0095(2)
As(1)	3*k*	0.15675(11)	0.44785(11)	1/2	0.0031(3)
As(2)	3*k*	0.19388(11)	0.26140(10)	1/2	0.0034(3)
As(3)	3*k*	0.37261(11)	0.48689(11)	1/2	0.0028(3)
As(4)	3*j*	0.27065(11)	0.07280(10)	0	0.0055(3)
As(5)	3*j*	0.44670(11)	0.28996(10)	0	0.0037(3)
As(6)	3*j*	0.48934(10)	0.11474(10)	0	0.0039(3)
As(7)	1*e*	2/3	1/3	0	0.0037(6)
As(8)	1*d*	1/3	2/3	1/2	0.0026(6)
As(9)	1*b*	0	0	1/2	0.0065(5)

[a] U_{eq} is defined as one-third of the trace of the orthogonalized $\mathbf{U}_{ij}$ tensor.

Possible space groups to be considered were those in Laue class 6/*m*. The centrosymmetric space group $P6_3/m$ was chosen first because it is the most common one adopted by many related hexagonal structures built of centered trigonal prisms. A model determined by direct methods could be refined with well-behaved anisotropic displacement parameters for all atoms, but only to $R(F) = 0.12$. The sites at (0, 0, 1/4) and (0, 0, 3/4) are partially occupied by As atoms, each coordinated by nine (symmetry equivalent) metal atoms in a tricapped trigonal prism. Because the distance between these sites is 1.7791(1) Å, equal to half the *c* parameter, the occupancy must be 50% (or less) to preclude unreasonable As−As contacts. On a local level, when an As atom occupies one of these sites, the three neighboring metal atoms capping the trigonal prism (i.e., "waist contact" atoms) are displaced away, whereas the six metal atoms at the corners of the trigonal prism move closer to attain reasonable metal−As bond distances. An additional disorder is thus introduced in which the position of the metal atoms forming the tricapped trigonal prism is split into two closely spaced sites, each occupied at 50%, as is frequently observed in related structures, such as $Cr_{12}P_7$.[15]

In space group $P6_3/m$, the symmetry equivalence of (0, 0, 1/4) and (0, 0, 3/4) (Wyckoff position 2*a*) obliges the occupying As atoms to be disordered over these sites. Transformation to the lower symmetry space group $P\bar{6}$ (through the group−subgroup relation $P6_3/m \xrightarrow{t2,\text{origin shift}+0,0,1/4} P\bar{6}$) allows an ordered model to be proposed because the As atoms can fully occupy either (0, 0, 0) (Wyckoff position 1*a*) or (0, 0, 1/2) (Wyckoff position 1*b*), which are independent sites. It is well recognized that this space group ambiguity plagues the accurate determination of many related hexagonal structures.[16] Refinements in

(12) (a) Engström, I. *Acta Chem. Scand.* **1965**, *19*, 1924. (b) Hyde, B. G.; Andersson, S. *Inorganic Crystal Structures*; Wiley: New York, 1989.
(13) Sheldrick, G. M. *SHELXTL*, version 5.1; Bruker Analytical X-ray Systems, Inc.: Madison, WI, 1997.
(14) *International Tables for X-ray Crystallography*; Wilson, A. J. C., Ed.; Kluwer: Dordrecht, The Netherlands, 1992; Vol. C.
(15) Chun, H. K.; Carpenter, G. B. *Acta Crystallogr., Sect. B: Struct. Crystallogr. Cryst. Chem.* **1979**, *35*, 30.

Table 3. Selected Interatomic Distances (Å) for Nb_9PdAs_7

Nb(1)−As(4)	2.600(1) (×2)	Nb(6)−As(1)	2.614(1) (×2)
Nb(1)−As(5)	2.629(2) (×2)	Nb(6)−As(2)	2.639(2) (×2)
Nb(1)−As(2)	2.667(2)	Nb(6)−As(4)	2.772(2)
Nb(1)−Nb(9)	3.048(2) (×2)	Nb(6)−Nb(2)	3.091(2) (×2)
Nb(1)−Nb(7)	3.211(2) (×2)	Nb(6)−Nb(9)	3.212(2)
Nb(1)−Nb(2)	3.288(2)	Nb(6)−Nb(8)	3.289(2)
Nb(1)−Nb(3)	3.340(2)	Nb(6)−Nb(5)	3.397(2)
Nb(1)−Nb(4)	3.379(2)	Nb(6)−Nb(7)	3.429(2)
Nb(1)−Pd	3.234(2)	Nb(6)−Pd	2.953(2) (×2)
Nb(2)−As(4)	2.617(2) (×2)	Nb(7)−As(2)	2.707(2) (×2)
Nb(2)−As(6)	2.623(1) (×2)	Nb(7)−As(9)	2.756(1) (×2)
Nb(2)−As(1)	2.732(2)	Nb(7)−As(4)	2.818(2)
Nb(2)−Nb(5)	3.029(2) (×2)	Nb(7)−Nb(1)	3.211(2) (×2)
Nb(2)−Nb(6)	3.091(2) (×2)	Nb(7)−Nb(6)	3.429(2)
Nb(2)−Nb(1)	3.288(2)	Nb(7)−Nb(9)	3.616(2)
Nb(2)−Nb(3)	3.320(2)	Nb(7)−Nb(7)	3.646(2) (×2)
Nb(2)−Nb(4)	3.381(2)	Nb(7)−Pd	2.940(2) (×2)
Nb(2)−Pd	3.222(2)	Nb(7)−Pd	2.981(2) (×2)
Nb(3)−As(6)	2.621(1) (×2)	Nb(8)−As(1)	2.622(2) (×2)
Nb(3)−As(5)	2.626(2) (×2)	Nb(8)−As(3)	2.624(1) (×2)
Nb(3)−As(7)	2.644(1) (×2)	Nb(8)−As(8)	2.643(1) (×2)
Nb(3)−Nb(2)	3.320(2)	Nb(8)−Nb(6)	3.289(2)
Nb(3)−Nb(4)	3.322(2)	Nb(8)−Nb(5)	3.305(2)
Nb(3)−Nb(4)	3.329(2)	Nb(8)−Nb(5)	3.325(2)
Nb(3)−Nb(1)	3.340(2)	Nb(8)−Nb(9)	3.339(2)
Nb(3)−Nb(3)	3.388(2) (×2)	Nb(8)−Nb(8)	3.386(2) (×2)
Nb(4)−As(5)	2.625(2) (×2)	Nb(9)−As(3)	2.630(1) (×2)
Nb(4)−As(6)	2.632(2) (×2)	Nb(9)−As(2)	2.635(2) (×2)
Nb(4)−As(3)	2.737(2)	Nb(9)−As(5)	2.744(2)
Nb(4)−Nb(9)	3.043(1) (×2)	Nb(9)−Nb(4)	3.043(1) (×2)
Nb(4)−Nb(5)	3.072(1) (×2)	Nb(9)−Nb(1)	3.048(2) (×2)
Nb(4)−Nb(3)	3.322(2)	Nb(9)−Nb(6)	3.212(2)
Nb(4)−Nb(3)	3.329(2)	Nb(9)−Nb(8)	3.339(2)
Nb(4)−Nb(1)	3.379(2)	Nb(9)−Nb(5)	3.404(2)
Nb(4)−Nb(2)	3.381(2)	Nb(9)−Nb(7)	3.616(2)
Nb(5)−As(3)	2.630(1) (×2)	Pd−As(4)	2.538(1) (×2)
Nb(5)−As(1)	2.632(2) (×2)	Pd−As(9)	2.561(1)
Nb(5)−As(6)	2.750(2)	Pd−As(2)	2.662(2)
Nb(5)−Nb(2)	3.029(2) (×2)	Pd−Nb(7)	2.940(2) (×2)
Nb(5)−Nb(4)	3.072(1) (×2)	Pd−Nb(6)	2.953(2) (×2)
Nb(5)−Nb(8)	3.305(2)	Pd−Nb(7)	2.981(2) (×2)
Nb(5)−Nb(8)	3.325(2)	Pd−Nb(2)	3.222(2)
Nb(5)−Nb(6)	3.397(2)	Pd−Nb(1)	3.234(2)
Nb(5)−Nb(9)	3.404(2)		

$P\bar{6}$ clearly supported an ordered model in which only the (0, 0, $^1/_2$) site is occupied by the As(9) atom, which centers a tricapped trigonal prism as mentioned earlier. Moreover, the corners of the trigonal prism, assigned as Nb(7), are distinguishable from the capping atoms, assigned as Pd. In accordance with the calculated Flack parameter of 0.45(3), the structure was refined as a racemic twin.

The final refinement gave $R(F) = 0.0328$ and $R_w(F_o^2) = 0.0728$, with reasonable anisotropic displacement parameters for all atoms. The two twin domains are present at 47(2) and 53%. The final difference electron density map is featureless ($\Delta\rho_{max} = 2.16$, $\Delta\rho_{min} = -1.99$ e$^-$ Å^{-3}). The atomic positions of Nb_9PdSb_7 were standardized with the program STRUCTURE TIDY.[17] Final values of the positional and displacement parameters are given in Table 2. Selected interatomic distances are listed in Table 3. Further data in the form of a CIF file are available as Supporting Information, and final structural amplitudes are available from the authors.

Electrical Resistivity. A single crystal of dimensions 0.025 × 0.0025 × 0.0025 cm was mounted in a two-probe configuration for an ac resistivity measurement along the crystallographic *c* (needle) axis between 2 and 300 K on a Quantum Design PPMS system equipped with an ac-transport controller (Model 7100). A current of 0.1 mA and a frequency of 16 Hz were used.

Band Structure. A tight-binding extended Hückel band structure calculation was performed on Nb_9PdAs_7 with use of the EHMACC suite of programs.[18,19] The atomic parameters were taken from literature values and are listed in Table 4. Properties were extracted from the band structure using 80 *k* points in the irreducible portion of the Brillouin zone.

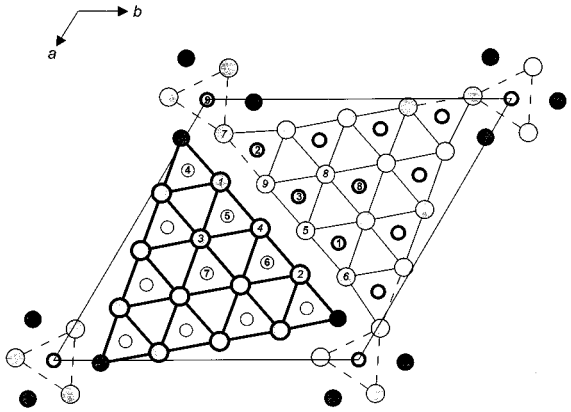

Figure 1. Structure of Nb_9PdAs_7 viewed in projection down the *c* axis. The large, lightly shaded circles are Nb atoms, the medium solid circles are Pd atoms, and the small open circles are As atoms. Atoms at $z = 0$ have thin rims and those at $z = ^1/_2$ have thick rims. The dashed lines are Nb−Nb contacts longer than 3.5 Å.

Table 4. Extended Hückel Parameters

atom	orbital	H_{ii} (eV)	ζ_{i1}	c_1	ζ_{i2}	c_2
Nb	5s	−9.04	1.89			
	5p	−5.13	1.85			
	4d	−9.94	4.08	0.6401	1.64	0.5516
Pd	5s	−7.51	2.19			
	5p	−3.86	2.15			
	4d	−12.53	5.98	0.55	2.61	0.67
As	4s	−16.22	2.23			
	4p	−12.16	1.89			

Results and Discussion

Structure. About 18 compounds have been discovered to date in the (Nb, Ta)−(Ni, Pd, Pt)−(P, As, Sb) systems,[4] but Nb_9PdAs_7 is the first ternary niobium palladium arsenide and is isostructural to none of them. Its structure type is new. In common with most ternary metal-rich phosphides and arsenides, it is characterized by a short axis between 3 and 4 Å in the unit cell ($c = 3.5582(1)$ Å) and uses pnicogen-centered trigonal prisms as structural building blocks. A projection of the structure viewed along the short *c* axis is shown in Figure 1. All atoms are located either on $z = 0$ (light lines) or $z = ^1/_2$ planes (heavy lines). The As-centered trigonal prisms share corners within the *ab* plane to form larger triangular assemblies and share faces along the *c* direction to form infinite columns, $^1_\infty[Nb_{15}As_{10}]$ and $^1_\infty[Nb_{12}Pd_3As_{10}]$. Neighboring columns are displaced relative to each other by $^1/_2\,\vec{c}$. Additional As atoms (As(9)) occupy tricapped trigonal prismatic sites generated along the *c* axis. The representation in Figure 1 emphasizes the As-centered trigonal prismatic building blocks and shows only the metal−metal contacts that make up their edges (the dashed lines indicate Nb−Nb contacts longer than 3.5 Å). There are metal−As and metal−metal bonds within and between the columnar assemblies that are also important but not shown. Along the *c* direction, each atom is 3.5582(1) Å away from its symmetry equivalent above and below; this distance is too far to be considered bonding, even for Nb atoms (the largest among Nb, Pd, and As). In the following discussion, we consider only those Nb−Nb contacts shorter than 3.5 Å to be bonding.

(16) Jeitschko, W.; Jakubowski-Ripke, U. *Z. Kristallogr.* **1993**, *207*, 69.
(17) Gelato, L. M.; Parthé, E. *J. Appl. Crystallogr.* **1987**, *20*, 139.
(18) Whangbo, M.-H.; Hoffmann, R. *J. Am. Chem. Soc.* **1978**, *100*, 6093.
(19) Hoffmann, R. *Solids and Surfaces: A Chemist's View of Bonding in Extended Structures*; VCH Publishers: New York, 1988.

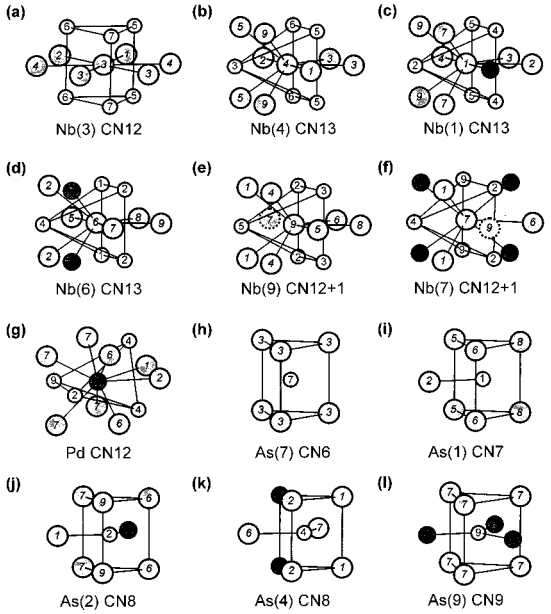

Figure 2. Representative coordination polyhedra in Nb_9PdAs_7. The large, lightly shaded circles are Nb atoms, the medium solid circles are Pd atoms, and the small open circles are As atoms. The broken circles in (e) and (f) indicate a Nb atom further than 3.5 Å away from the coordination center.

While similar, the two types of columns, $^1_\infty[Nb_{15}As_{10}]$ and $^1_\infty[Nb_{12}Pd_3As_{10}]$, are chemically distinguishable in that Pd atoms preferentially occupy the corners of the triangular assembly in the latter. Between corresponding atoms in these two types of columns, the metrical details are comparable for atoms in the interior, but they deviate significantly for atoms at the periphery and especially at the corners. Although the interatomic distances are generally unexceptional (Table 3), there are important distortions for bonds involving atoms near the *c* axis. Representative coordination polyhedra are shown in Figure 2.

The Nb atoms occupy nine crystallographically inequivalent sites. They can be classified into three categories: (i) "interior" Nb(3) and Nb(8), (ii) "peripheral" Nb(1), Nb(2), Nb(4), Nb(5), Nb(6), and Nb(9), and (iii) "corner" Nb(7) atoms. Figure 2(a) shows that the coordination of an "interior" atom such as Nb(3) is anticuboctahedral (CN12), with three As atoms above, three As atoms below, and six Nb atoms in the same plane in an *hcp* arrangement. The slip of the $^1_\infty[Nb_{15}As_{10}]$ and $^1_\infty[Nb_{12}Pd_3As_{10}]$ columns by $^1/_2\,\vec{c}$ causes the "peripheral" atoms to attain CN13. Each such Nb atom is surrounded by five As atoms (arranged in a square pyramid) and eight metal atoms, among which are zero, one, or two Pd atoms (Figure 2(b)−(d)). Nb(9) is distinctly different in that one of the coordinating atoms (Nb(7), plotted as a broken circle in Figure 2(e)) is significantly further away (3.616(2) Å, shown as a dashed line in Figure 1). This arises because Nb(7) must be displaced toward As(9) on the *c* axis to form reasonable Nb(7)−As(9) bonds (2.756(1) Å). Finally, the "corner" Nb(7) atom itself has quite a different coordination from the others; it is surrounded by five As, four Pd, and three (and one more distant) Nb atoms, giving CN12+1 (Figure 2(f)).

The Pd atoms at the corners of the $^1_\infty[Nb_{12}Pd_3As_{10}]$ columns are located at the only sites in the structure where a tetrahedral environment of As atoms is available (Figure 2(g)), which is consistent with the coordination preference of essentially zerovalent palladium (d^{10}). Eight more distant Nb atoms complete the CN12 coordination of Pd.

All As atoms occupy centers of trigonal prisms that have metal atoms at the vertexes and are capped by zero to three additional metal atoms on their quadrilateral faces to give CNs ranging from 6 to 9 (Figure 2(h)−(l)).

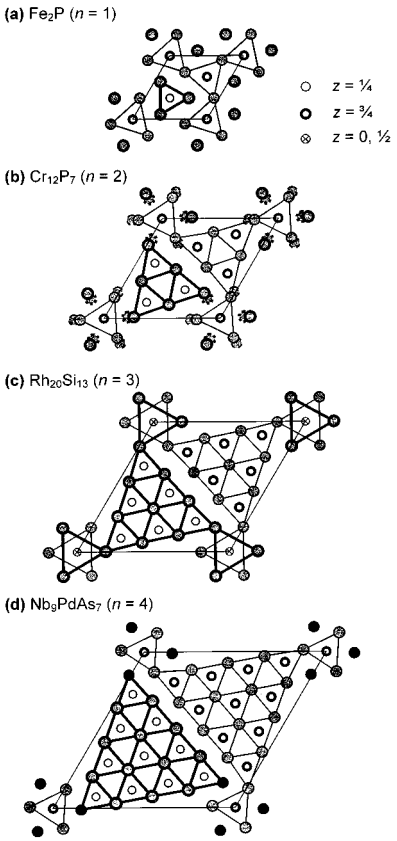

Figure 3. Comparison of members in the $M_{n^2+3n+2}X_{n^2+n}Y$ family, where transition metal atoms M are shown as shaded circles, and nonmetal or metalloid atoms X, Y = Si, P, As are shown as open circles. M atoms form trigonal prisms centered by X atoms; Y atoms are found along the *c* axis. Shown are the structures of (a) Fe_2P (origin shifted by ($^1/_3$, $-^1/_3$, $-^1/_4$)), (b) $Cr_{12}P_7$ (origin shifted by (0, 0, $^1/_2$)) (the arrangement of Cr atoms when P is at (0, 0, $^3/_4$) is highlighted; broken circles are the corresponding Cr positions when P is at (0, 0, $^1/_4$)), (c) $Rh_{20}Si_{13}$, and (d) Nb_9PdAs_7 (origin shifted by (0, 0, $^1/_4$)).

Structural Relationships. The hexagonal structure adopted by Nb_9PdAs_7 resembles those of a large family of metal-rich compounds, generally silicides, phosphides, and arsenides, composed of differently sized triangular columns of trigonal prisms.[12b,20] Nb_9PdAs_7 belongs to a structural series of general formula $M_{n^2+3n+2}X_{n^2+n}Y$, where typically M is a transition or rare-earth metal and X, Y are nonmetals or metalloids.[12] M resides at the corners of trigonal prisms, X at the center of trigonal prisms, and Y at the center of tricapped trigonal prisms, octahedra, or some irregular coordination polyhedra depending on where it is located along (0, 0, *z*). In our discussion, X and Y are the same element (Si, P, or As). The index *n* indicates the number of joined trigonal prisms along a basal edge of the triangular columns. Previously, only the three members corresponding to $n = 1$ (Fe_2P-type),[21] 2 ($Cr_{12}P_7$-type),[15] and 3 ($Rh_{20}Si_{13}$-type)[12a] were known. Nb_9PdAs_7 is the first member discovered with $n = 4$, having triangular columns with the longest edge so far (other than $n = \infty$, corresponding to the WC-type structure)[22] in this series. The structures with $n = 1$, 2, 3, and 4 are shown in Figure 3.

(20) Pearson, W. B. *The Crystal Chemistry and Physics of Metals and Alloys*; Wiley: New York, 1972.
(21) Rundqvist, S.; Jellinek, F. *Acta Chem. Scand.* **1959**, *13*, 425.
(22) Butorina, L. N. *Sov. Phys. Crystallogr. (Engl. Transl.)* **1960**, *5*, 216.

The positions of the Y atoms differ in these four structures. For ease of comparison, origin shifts were applied so that tricapped trigonal prismatic sites are located at (0, 0, $^1/_4$) or (0, 0, $^3/_4$) and octahedral sites at (0, 0, 0) or (0, 0, $^1/_2$). In Fe_2P ($P\bar{6}2m$),[21] the two tricapped trigonal prismatic sites are crystallographically inequivalent, and only one of these is occupied by P atoms (Figure 3(a)). In $Cr_{12}P_7$ ($P6_3/m$),[15] the two tricapped trigonal prismatic sites are crystallographically equivalent and are only 50% occupied by P atoms to preclude unrealistically short P−P contacts of ∼1.65 Å. Depending on which of these sites is occupied on a local level, the surrounding Cr atoms will adjust their positions so that the three capping or waist atoms are pushed away and the six atoms at the corners of the trigonal prism are drawn toward the P center. Thus, the $Cr_{12}P_7$ structure, when refined in space group $P6_3/m$, is portrayed as an averaged structure (Figure 3(b)). In $Rh_{20}Si_{13}$ ($P6_3/m$),[12a] the two octahedral sites are crystallographically equivalent and are also only 50% occupied by Si atoms (Figure 3(c)). Unlike the case of $Cr_{12}P_7$, however, there is no need for a distortion involving the positions of Rh atoms coordinating the Si atoms because the Rh−Si contacts are already reasonable. More complicated situations arise in which both the tricapped trigonal prismatic and octahedral sites are partially occupied in a random manner, such as occurs in $Rh_{12}As_7$.[23] In Nb_9PdAs_7 ($P\bar{6}$), only the tricapped trigonal prismatic site at (0, 0, $^1/_4$) is occupied by As atoms (Figure 3(d)). The difference in the capping atoms (Pd) and the atoms at the corners of the trigonal prism (Nb(7)) of this tricapped trigonal prismatic site is a unique feature of Nb_9PdAs_7. This arrangement anchors the position of the As atom so that an ordered structure can be refined in space group $P\bar{6}$. As a consequence, one of the large triangular columns $^1_\infty[Nb_{12}Pd_3As_{10}]$ has Pd atoms at the corners, whereas the other column $^1_\infty[Nb_{15}As_{10}]$ does not. The extreme case of $n = \infty$ in the $M_{n^2+3n+2}X_{n^2+n}Y$ series gives the WC structure, with C atoms occupying the centers of half the trigonal prisms made up of W atoms at the corners (or vice versa).

In the $M_{n^2+3n+2}X_{n^2+n}Y$ series, only half of the trigonal prisms are filled, and half of the tricapped trigonal prismatic or octahedral sites along (0, 0, z) are filled. Filling all these sites generates another structural series with general formula $M_{n^2+3n+2}X_{2n^2}Y_2$,[12b] adopted mostly by RE−Ni−Si phases, such as $Ce_6Ni_2Si_3$ ($n = 2$), $La_5Ni_2Si_3$ ($n = 3$), $La_{15}Ni_7Si_{10}$ ($n = 4$), and $La_{21}Ni_{11}Si_{15}$ ($n = 5$);[24,25] the AlB_2 structure ($n = \infty$) corresponds to the extreme case. Whether other members of the $M_{n^2+3n+2}X_{n^2+n}Y$ series can be synthesized remains an open question. The next largest member ($n = 5$), with hypothetical formula $M_{42}X_{30}Y$, is worth targeting. There do exist related hexagonal structures containing even larger triangular columns, with six ($Ho_{20}Ni_{66}P_{43}$)[26] or seven ($La_{18}Rh_{96}P_{51}$)[27] joined trigonal prisms along a basal edge. They have complicated atomic arrangements that cannot be fit into a general formula.

Bonding. There are strong metal−metal and metal−As but no As−As bonding interactions in the structure. Because all As atoms are isolated and surrounded by more electropositive Nb atoms, they can be assigned a formal oxidation state of −3 according to the Zintl concept. What to assign as an initial charge for Pd is less obvious because of its closeness in electronegativity to As; indeed, in similar cases such as Sc_2Ni_2In[28] or TiNiSi,[29] it can be argued that the late transition metal (Ni) attains a negative charge. With a preponderance of the more electropositive Nb atoms within the structure, it is reasonable to assume that most of the electron transfer will occur from Nb to As, and not between Pd and As. If we assume a d^{10} configuration for the Pd atoms, we arrive at the formulation $[(Nb^{2.33+})_9(Pd^0)(As^{3-})_7]$. In this crude approximation, each Nb atom donates 2.33 valence electrons to form strong Nb−As bonds. The remaining 2.67 valence electrons on each Nb atom are then available for forming metal−metal bonds (mostly Nb−Nb but also some Nb−Pd), which is consistent with the extended network of Nb−Nb contacts of 3.029(2)−3.429(2) Å observed in the structure of Nb_9PdAs_7. These metal−metal bonds are crucial in stabilizing the structure.

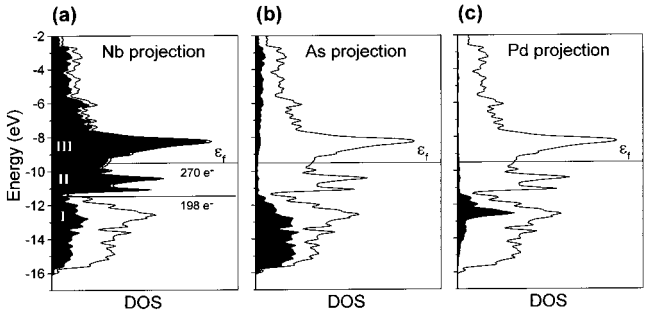

Figure 4. Contributions of (a) Nb, (b) As, and (c) Pd (shaded regions) to the total density of states (DOS) (line) for Nb_9PdAs_7. See text for discussion of regions **I**, **II**, **III**, and electron count shown in (a). The Fermi level, ϵ_f, lies at −9.5 eV, at a count of 270 e^- per unit cell.

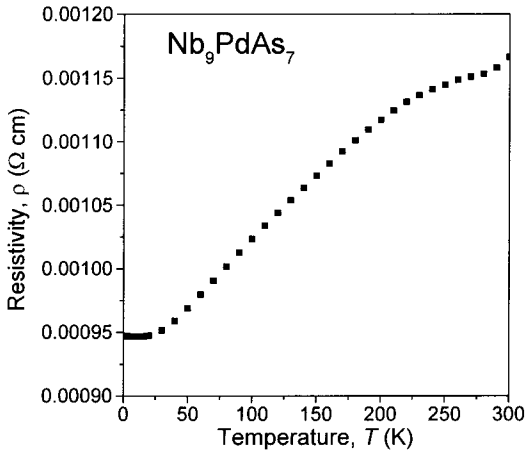

Figure 5. Temperature dependence of the resistivity along the needle axis c of a single crystal of Nb_9PdAs_7.

To analyze the bonding in more detail, the band structure of Nb_9PdAs_7 was calculated. The density of states (DOS) is plotted in Figure 4. As expected for this metal-rich compound, there is no band gap at the Fermi level ($\epsilon_f = -9.50$ eV), which is also consistent with the metallic behavior of Nb_9PdAs_7 ($\rho_{300} = 1.17 \times 10^{-3}$ Ω cm; $\rho_{300}/\rho_2 = 1.24$) seen in the resistivity plot in Figure 5. The states around the Fermi level are dominated by Nb 4d contributions (Figure 4(a)), implying that electronic conduction occurs largely through the extended network of metal−metal bonded Nb atoms. The Nb 4d states are broadly dispersed and can be roughly divided into three regions,

(23) (a) Lambert-Andron, B.; Dhahri, E.; Chaudoüet, P.; Madar, R. *J. Less-Common Met.* **1985**, *108*, 353. (b) Pivan, J. Y.; Guérin, R.; Sergent, M. *J. Less-Common Met.* **1985**, *107*, 249.
(24) Bodak, O. I.; Gladyshevskii, E. I.; Kharchenko, O. I. *Sov. Phys. Crystallogr. (Engl. Transl.)* **1974**, *19*, 45.
(25) Prots, Yu. M.; Jeitschko, W. *Z. Kristallogr. Suppl.* **1997**, *12*, 137.
(26) Pivan, J.-Y.; Guérin, R.; Sergent, M. *Mater. Res. Bull.* **1985**, *20*, 887.
(27) Pivan, J.-Y.; Guérin, R.; Pena, O.; Padiou, J.; Sergent, M. *Mater. Res. Bull.* **1988**, *23*, 513.
(28) Pöttgen, R.; Dronskowski, R. *Z. Anorg. Allg. Chem.* **1996**, *622*, 355.
(29) Landrum, G. A.; Hoffmann, R.; Evers, J.; Boysen, H. *Inorg. Chem.* **1998**, *37*, 5754.

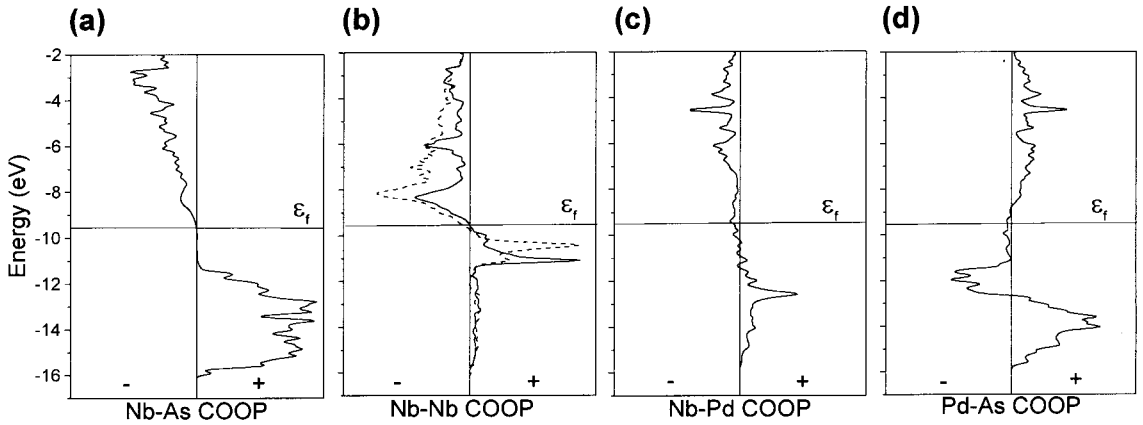

Figure 6. Crystal orbital overlap population (COOP) curves for (a) Nb−As, (b) Nb−Nb (solid line, 3.029(2)−3.091(2) Å; dashed line, 3.212(2)−3.429(2) Å), (c) Nb−Pd, and (d) Pd−As interactions in Nb_9PdAs_7.

separated by local minima: **I**, −16.0 to −11.4 eV; **II**, −11.4 to −9.5 eV; **III**, above −9.5 eV. Most of the As 4p states lie between −16.0 and −11.4 eV (Figure 4(b)), which overlaps with region **I** of the Nb 4d states. The substantial mixing of Nb and As states in this region leads to strong Nb−As covalent bonds. This expectation is confirmed by the crystal orbital overlap population (COOP)[30] curve in Figure 6(a), which shows that Nb−As bonding is optimized with all bonding levels and no antibonding levels occupied (Mulliken overlap population (MOP) of 0.393). The Nb−As bond distances of 2.600(1)−2.818(2) Å in Nb_9PdAs_7 are similar to those in $NbAs_2$ (2.53−2.82 Å)[31] and Nb_4As_3 (2.545(2)−2.752(2) Å).[32]

Between −11 and −7 eV, the DOS is dominated by Nb 4d states, with a local minimum near the Fermi level separating regions **II** and **III**. Region **II** is associated with Nb−Nb bonding levels and region **III** with Nb−Nb antibonding levels, as verified by inspection of the Nb−Nb COOP curve (Figure 6(b)). Most of the Nb−Nb distances *between* the large triangular columns (3.029(2)−3.091(2) Å) are actually shorter than those *within* columns (3.212(2)−3.429(2) Å), notwithstanding the portrayal in Figure 1. The intercolumn Nb−Nb bonds are exactly optimized, with the Nb−Nb bonding levels completely filled and the Nb−Nb antibonding levels completely empty (solid line in Figure 6(b)); the MOP of 0.21 represents fairly strong metal−metal interactions. The intracolumn Nb−Nb bonds are also nearly optimized, with only a small portion of the antibonding levels occupied (dashed line in Figure 6(b)); the slightly smaller MOP of 0.13 indicates weaker but still substantial metal−metal interactions. All Nb−Nb bonds found in Nb_9PdAs_7 are greater than the 2.86 Å bond found in elemental Nb (which also has longer 3.30 Å contacts)[33] but are comparable to those in other Nb-rich arsenides, such as Nb_4As_3 (2.905(1)−3.487(2) Å).[32]

The oxidation state formulation $[(Nb^{2.33+})_9(Pd^0)(As^{3-})_7]$ suggests that per unit cell ($Z = 3$), 198 valence electrons ($10 \times 1 \times 3 + 8 \times 7 \times 3 = 198$) are needed to fill up metal−As bonding levels, and the remaining 72 valence electrons ($2.67 \times 9 \times 3 = 72$) will then be used to fill up Nb−Nb bonding levels. This crude analysis is nicely validated by the band structure calculation. At a count of 198 electrons, the DOS curve is filled up to −11.39 eV, precisely at the local minimum separating region **I** (Nb−As bonding) from regions **II** (Nb−Nb bonding) and **III** (Nb−Nb antibonding) in the Nb d-block (Figure 4(a)).

The contribution of the Pd 4d states falls essentially in the narrow peak below the Fermi level between −12 and −13 eV (Figure 4(c)), which is also consistent with the d^{10} configuration proposed in the oxidation state formulation above. The location of Pd atoms at the corner sites, where they are coordinated in a tetrahedral environment of As atoms, is thus understandable; any of the other metal sites within the triangular assemblies are of lower symmetry and would be less preferred by a d^{10} species. An MOP of 0.069 reveals weak heteroatomic Nb−Pd bonds (Figure 6(c)) of 2.940(2)−2.981(2) Å, which are longer than the sum of Pauling single-bond radii ($r_{Nb} + r_{Pd} = 1.342 + 1.278$ Å $= 2.620$ Å).[34] As expected for a closed shell d^{10} configuration for Pd, some Pd−As antibonding levels are located below the Fermi level. Although small, the cumulative MOP of 0.12 represents normal Pd−As interactions. The observed Pd−As bond distances of 2.538(1)−2.662(2) Å are comparable with those in $PdAs_2$ (2.50 Å)[35] and Pd_2As (2.39−2.70 Å).[36]

In conclusion, the first and rather unique ternary niobium palladium arsenide has been synthesized. The structure of Nb_9PdAs_7 not only extends the $M_{n^2+3n+2}X_{n^2+n}Y$ family of WC related hexagonal structures to $n = 4$, but also exhibits some features that are not observed in the other members in the same family. In particular, ordering of different metal atoms can occur even within these very large triangular columns of linked trigonal prisms, so that the Pd atoms prefer sites of tetrahedral As coordination. Other related members with smaller or larger triangular assemblies should be feasible to target. The band structure calculation shows that the bonding of even metal-rich compounds can be understood to a first approximation by simple chemical ideas, such as the Zintl concept.

Acknowledgment. This work was supported by the Natural Sciences and Engineering Research Council of Canada and the University of Alberta. We thank Dr. Robert McDonald (Faculty Service Officer, X-ray Crystallography Laboratory) for the X-ray data collection and Ms. Christina Barker (Department of Chemical and Materials Engineering) for assistance with the EDX analyses.

Supporting Information Available: An X-ray crystallographic file in CIF format for the structure of Nb_9PdAs_7. This material is available free of charge via the Internet at http://pubs.acs.org.

IC010544H

(30) Hughbanks, T.; Hoffmann, R. *J. Am. Chem. Soc.* **1983**, *105*, 3528.
(31) Furuseth, S.; Kjekshus, A. *Acta Crystallogr.* **1965**, *18*, 320.
(32) Carlsson, B.; Rundqvist, S. *Acta Chem. Scand.* **1971**, *25*, 1972.
(33) Donohue, J. *The Structures of the Elements*; Wiley: New York, 1979.
(34) Pauling, L. *The Nature of the Chemical Bond*, 3rd ed.; Cornell University Press: Ithaca, NY, 1960.
(35) Brese, N. E.; von Schnering, H. G. *Z. Anorg. Allg. Chem.* **1994**, *620*, 393.
(36) Bälz, U.; Schubert, K. *J. Less-Common Met.* **1969**, *19*, 300.